Verification and Validation

Stiffener Flexural-Torsional Buckling

June 11, 2010

Table of Contents

1 Summary

Flexural-torsional stiffener buckling refers to a coupled buckling mode observed for stringer-stiffened panels where bending of the stringer section is accompanied by a twist. HyperSizer implements two methods to calculate the flexural-torsional buckling ***(FTB)*** load. One is based on a method developed by Argyris (1954), and the other is based on a procedure developed by Levy (1948). A detailed description for both of these methods can be found in the HyperSizer methods and equations document (HME) for flexural-torsional buckling (AID 016).

This document provides both verification and validation of these methods. HyperSizer method implementations are verified by comparing HyperSizer results with published results of equivalent methods. Verification is also performed by comparing HyperSizer solutions with finite element analyses to explore the solution accuracy over a broad design space. Validation compares HyperSizer results to publicly available experimental results.

The example problems are selected to represent the various design variations used in industry. The example problems include cases where the skin is relatively thick and initial buckling does not occur before FTB, as well as thin skin examples where the post buckled skin is included in the FTB analysis. Often, but not always, skin local buckling mode shapes provide geometric stiffening and increase the FTB load. Metallic and composite materials are included as well as panel concepts with different cross sectional shapes such as Zee, C, and I.

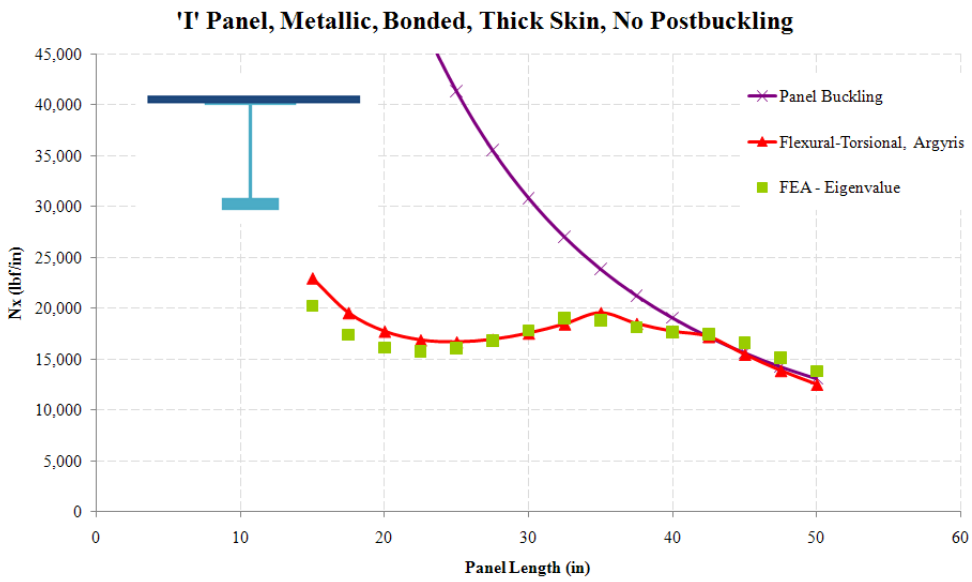

Figure 1 - Sample FEA verification results for a bonded, I stiffened panel.

2 Verification Ex 1: Argyris published soln, 'L' panel, metallic, postbuckling

Database: HyperSizer ANALYSIS METHODS 5.9.hdb
Project: Buckling Flexural-Torsional HVV
Group: 1: Argyris published soln, 'L' panel, metallic, postbuckling

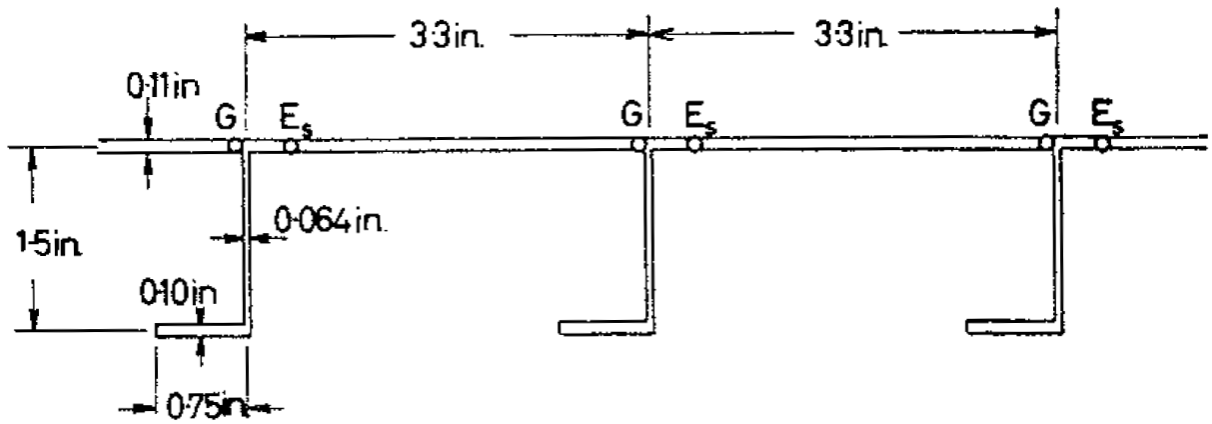

The original Argyris paper provided two sets of example calculations. Example 1 will be studied to verify the HyperSizer implementation of the Argyris method. Panel dimensions, loading, and material properties are listed in the tables below. The panel consists of a relatively thick facesheet with integral L-stiffeners. The results discussed are for the case where L = 22" (corresponds to $\lambda/\pi = 7$ in the original paper).

H	1.605"
S_x	3.3"
w_{flange}	0.782" = (.75"+.064"/2)
t_{flange}	0.10"
t_{web}	0.064"
$t_{facesheet}$	0.11"
L	22"

Material	E (Msi)	G (Msi)
Aluminum Alloy	10.0	3.85

HyperSizer was setup to use the same method as Argyris to calculate the local buckling stress of the panel by treating the stiffener spacing span as a simply supported plate. Argyris applies a factor of 1.12 to the final result. The same factor was applied in HyperSizer by defining a local buckling knockdown of 1.12 in the Buckling tab.

Results from the original paper are compared with HyperSizer results in Table 1. Levy method results are not reported because this is a thick-skinned panel (relative to the stringer).

Table 1 – HyperSizer and hand analysis results for Argyris (1954) Example 1. Levy method needs thick skin corrections.

		FTB Buckling Load (psi)	
	Local Skin Buckling Stress (psi)	**Postbuckling Considered**	**Postbuckling not Considered**
Published Result Argyris	45,000	43,200	51,100
HyperSizer Argyris	45,100	48,100	54,500

The discrepancy between the Hypersizer-Argyis and the results of the Argyris paper results requires further explanation.

Key Differences: Argyris Published Results vs. HyperSizer, Argyris

1. HyperSizer applies effective width expressions to describe the relationship between the postbuckled edge stress and the average stress. Argyris applies an experimentally derived linear relationship. See Figure 2.
2. Argyris does not iterate postbuckled solutions to convergence.
3. Argyis ignores $(1-\nu^2)^{-1}$ term in spring stiffness expressions leading a 10% reduction in spring stiffness.
4. Argyis models the web depth from the mean line of the skin. This adds a significant conservatism to the solutions as compared to HyperSizer. See Figure 3.

For stresses above the skin local buckling stress, the skin effective areas must be determined by iteration. Argyris assumes a linear relationship between the average stress and edge stress in the postbuckled skin where HyperSizer uses a more general effective width relationship. Figure 2 shows a comparison between the two methods. They happen to be in good agreement for this example.

In Argyris' calculations no iteration is performed – a critical stress level of 50 ksi is simply assumed. The author does mention that the stress values should be corrected after recalculating the effective skin area but then notes that "such refinement may be ignored here." HyperSizer always iterates to convergence. This discrepancy does not have much impact on the results for this example.

A major difference between the two methods is that Argyis ignores the Poisson's ratio term while calculating the torsional spring stiffness of the plate and stringer. The author states this fact in item (6) of the section 8 preface. Assuming a Poisson's ratio of 0.3, ignoring these terms leads to a 10% reduction in the spring stiffness terms.

The <u>most significant source of discrepancy</u> between the two calculations is how the web height is modeled. A schematic of the two modeling methods are shown in Figure 3. In the HyperSizer implementation, the reference axes are set at the bottom of the skin in order to consistently model stiffeners with and without attached flanges. Argyis sets the reference axis at the mean line of the skin and extends the web height to this reference axis. In physical terms, as compared to HyperSizer, the Argyris approach makes the web taller and thus more prone to tipping. Therefore the Argyris solutions will tend to appear more conservative than HyperSizer.

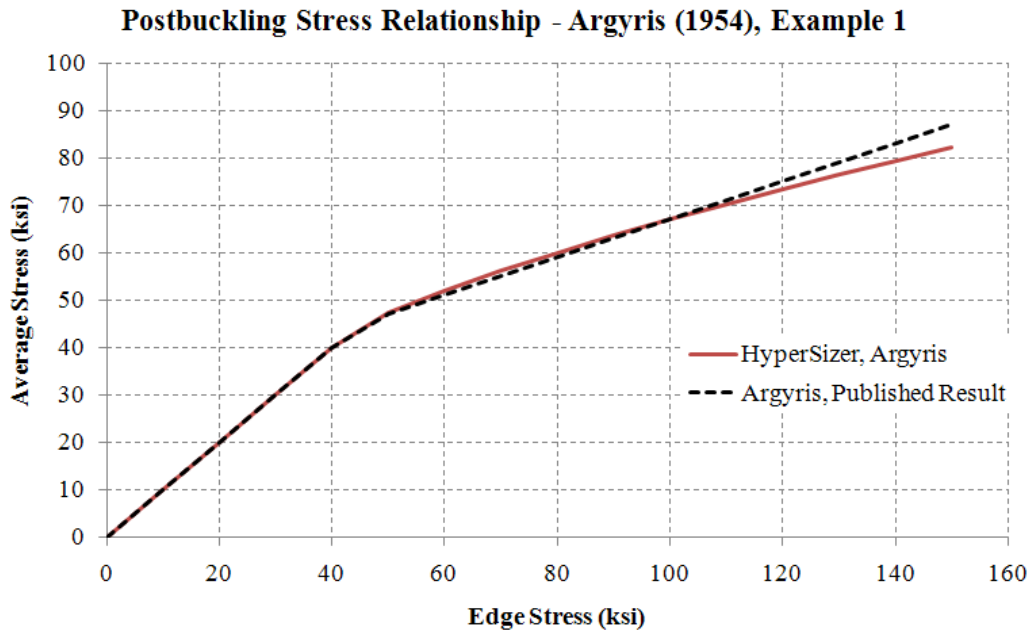

Figure 2 - Postbuckling stress relationships assumed by HyperSizer and the Argyris published calculations for the Example 1 L Panel. Argyris assumes a linear relationship while HyperSizer uses on effective width calculation.

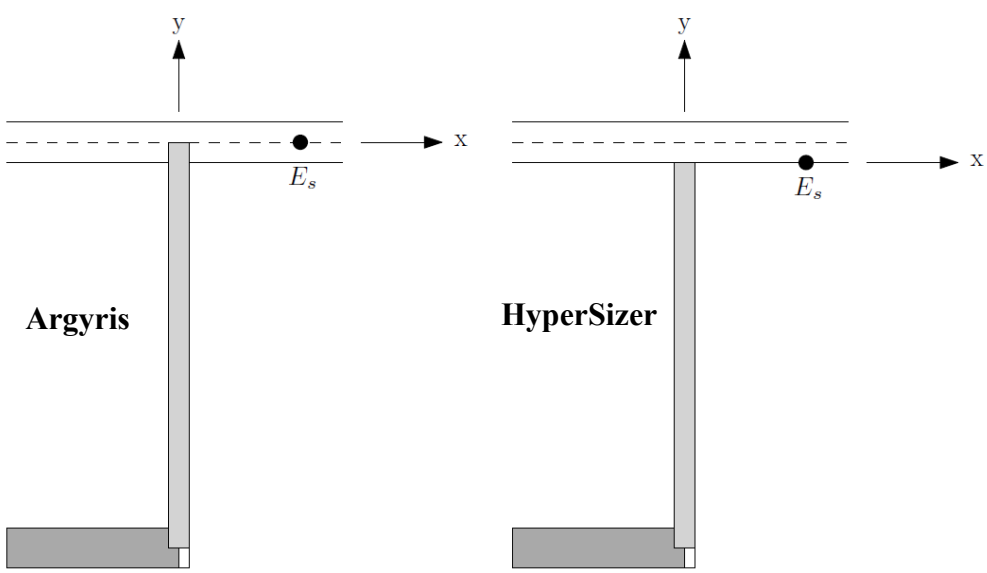

Figure 3 - Cross-section modeling differences between Argyis and HyperSizer. Argyris extends the web to the mean line of the skin. The Argyris x-x reference is also at the mean line of the skin. HyperSizer terminates the web at the bottom of the skin and its x-x reference is also at this location.

3 Verification Ex 2: Levy published soln, 'C' panel metallic, postbuckling

Database: HyperSizer ANALYSIS METHODS 5.9.hdb
Project: Buckling Flexural-Torsional HVV
Group: 3: Levy published soln, 'C' panel metallic, postbuckling

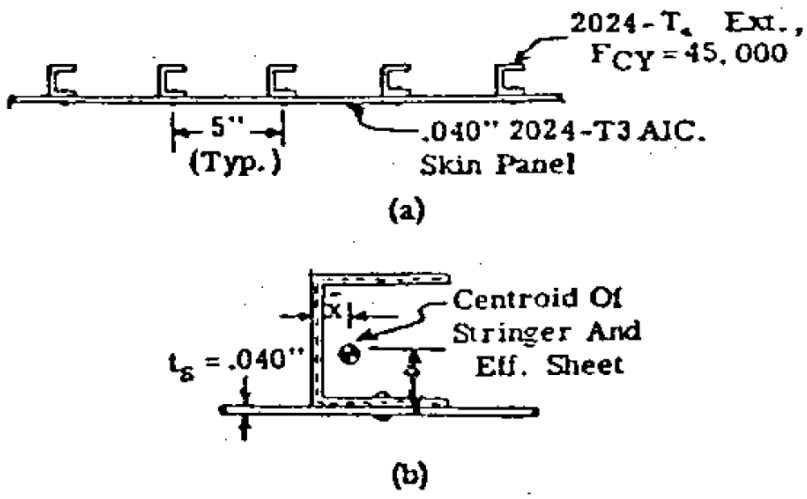

The following is an example problem found in the McCombs text *Engineering Column Analysis* on page 12.17. The McCombs text analyzes this panel for flexural-torsional stiffener buckling using the Levy method. This example is used to verify the HyperSizer implementation of the Levy method.

The panel is aluminum, fastened, thin-skinned, and composed of C-section stiffeners. Panel dimensions and material properties are found in the tables below. This panel was modeled in HyperSizer using the bonded C panel concept. The Levy method makes no special assumptions for bonded or fastened panels so this difference will not impact the results comparison.

H	2.14"
S_x	5"
w_{flange}	2.05"
t_{flange}	0.10"
t_{web}	0.10"
t_{skin}	0.04"
L	50"

Material	E (Msi)	G (Msi)
Aluminum Alloy	10.5	4.0425

Results from McCombs are compared with HyperSizer results in Table 2. HyperSizer Argyris method results are included. A comparison of the critical loads shows that the HyperSizer result matches the McCombs method almost exactly. The McCombs solution assumes that the panel is local buckled, but does not report a local buckling stress. Both the McCombs solution and the HyperSizer implementation of the Levy method handle the postbuckled calculations in the same manner by simply setting the effective plate area to half of its original value.

	Local Skin Buckling Load (psi)	**FTB Buckling Load (psi) Postbuckling Considered**
Published McCombs, Levy	N/a	14,800
HyperSizer, Levy	11,800	14,800
HyperSizer, Argyris	11,800	12,600

Table 2 – Comparison of results for McCombs example C panel. No local buckling load was specified in the McCombs solution. It makes no difference due to the way postbuckling is treated in the Levy method.

4 FEA Verification Process

HyperSizer has a feature called HyperFemGen that generates finite-element (FE) models of flat or curved panels with discretely mesh stiffeners using shell elements. This feature was used to generate FE models to verify the HyperSizer flexural-torsional failure methods. Please refer to the HyperFemGen user manual for a more detailed discussion on this feature.

For cases where stiffener buckling was the initial instability, a linear eigenvalue analysis was used to verify the method. This was typically the case for thick-skinned panels. For thin-skinned panels where local buckling (initial instability) occurred before stiffener buckling, a non-linear FEA postbuckling analysis was performed. All load cases with uniaxial compression.

For panel types with attached flanges, the connection was modeled as bonded. Future studies will incorporate FE modeling techniques to simulate fastened or riveted connections. Lynch et al. (2004) found that modeling riveted flanges as bonded can lead to non-conservative collapse loads of about 10% as compared to test (Al-2024 bulbed Tee sections).

The following section will described the boundary conditions used in the eigenvalue and geometric non-linear analysis. The traditional HyperSizer panel coordinate system is used to describe the applied boundary conditions. The x-axis corresponds to the longitudinal axis of the stiffeners (N_x). And the z-axis points in the out-of-plane direction away from the stiffeners.

4.1 Eigenvalue Analysis

For general linear eigenvalue analysis, two sets of boundary conditions are applied: one for the static load (perturbation load pattern) and another for the buckling boundary conditions. The overall objective of the boundary conditions was to simulate an end-shortening load while having the panel buckle as if it were simply supported on all sides.

Figure 4 shows the perturbation load boundary conditions. Identical boundary conditions were applied on opposite edges. Loads were applied with applied nodal displacements on all external edges. Rotational constraints parallel to the plate edges were applied to prevent rotations due to unsymmetrical laminates and shell offsets. In other words, for static FEA load application, all loaded plate edges were clamped. A single translation constraint in the z-direction was applied at the most central node of the panel to prevent rigid body motion.

Figure 5 shows boundary conditions for the buckling solution. Because it is the buckling solution, no external loads are applied. All *facesheet* edges were simply-supported.

The stiffener buckling constraints in the buckling solution are critical because the method assumes that the stiffener cross-section at the end points are pinned. In the theory this means the cross-section cannot translate in the plane of the cross-section, and it cannot twist. However the cross-section is allowed to warp. To simulate this “pinned” constraint all nodes along the edge of the stiffener web and free flange were constrained in the y-direction.

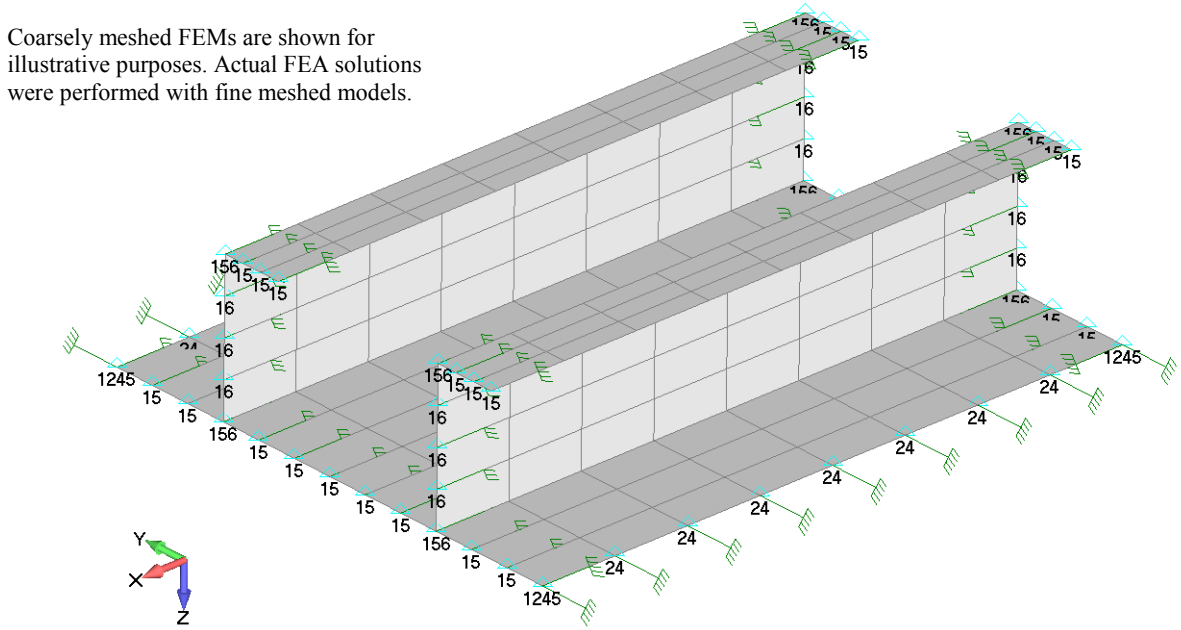

Figure 4 – Static (perturbation) boundary conditions for eigenvalue analysis. Loads were applied via enforced displacements (green lines). Rotational constraints were applied on the loaded plate edges.

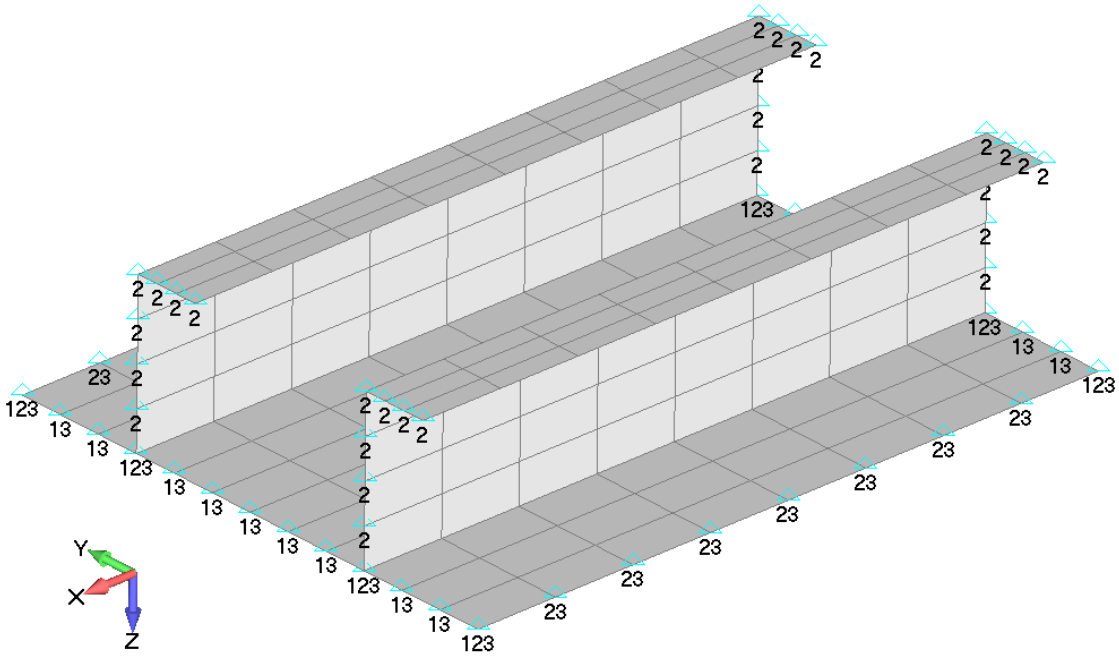

Figure 5 - Buckling boundary conditions for eigenvalue analysis. No rotational constraints were applied. On the short edge, T_x and T_z constraints were applied only to nodes attached to the skin. T_y constraints were applied on nodes exclusively attached to the edge of the stiffener web and free flange.

4.2 Geometric Non-Linear Postbuckling Analysis

Abaqus recommends three options for performing postbuckling and collapse analyses: non-linear quasi-static analysis, arc-length controlled methods such as Riks, and explicit dynamic analysis. Each method has different ways of handling critical points (bifurcation and limit) along the load displacement path. A detailed discussion of each method can be found in the NAFEMS publication.

Quasi-static analysis with artificial damping was used because it is better suited to handle localized instabilities than the Riks method and is more straightforward to perform than explicit analysis. This was also the approach taken in a FEA study performed by Lynch (2004).

Artificial damping was controlled via the dissipated energy fraction parameter. This parameter is the ratio of viscous energy to strain energy and is used to determine the artificial damping factor c. A dissipated energy fraction of 1×10^{-4} was used for all analyses unless specified as otherwise. This value is half of the Abaqus default. Sensitivity analyses have confirmed that this value is adequate for these types of problems. Geometric imperfections were applied to help the solution converge. In all reported cases, the imperfection applied was simply the first eigenmode from the linear analysis. The magnitude of the imperfection was always taken to be 10% of the facesheet thickness which is common rule-of-thumb for these types of analyses.

Figure 6 shows the boundary conditions used for the analysis. For the most part, the boundary conditions are a direct combination of the two sets of linear eigenvalue analysis boundary conditions described above. To simulate true flexural (panel) buckling, additional panels were modeled. The loaded edges of a single-bay model were constrained from rotation about the panel y-axis and applied x-displacements were used to introduce load. Multi-bay models mitigate this effect.

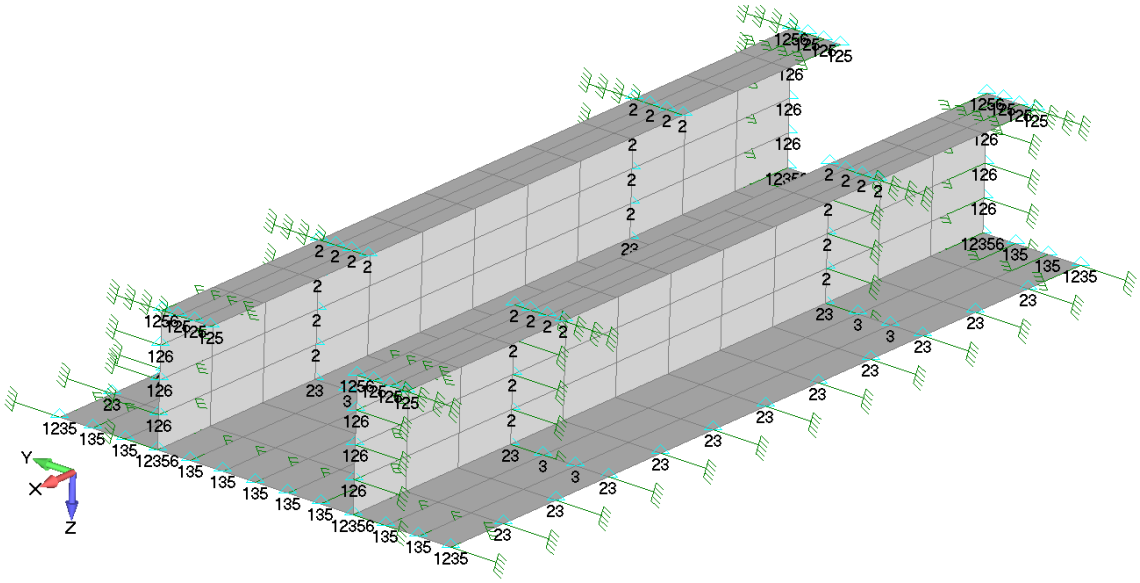

Figure 6 - Panel boundary conditions for quasi-static, geometrically non-linear analysis. A two-bay model is pictured though four-bay models were used. T_z constraints are applied on the bay-edge nodes attached to the skin. Applied T_y displacements are applied to the bay nodes attached to the web and free flange to force the torsional half-wave terminates at the bay-edge.

At each bay edge, translational z-constraints were applied to the facesheet nodes. The transverse edges were simply-supported. Applied y-displacement were applied to the web and free flange nodes at the bay edges to simulate the pinned boundary condition discussed previously.

5 Verification Ex 3: FEA, 'L' Panel, Composite, Thick Skin, No Postbuckling

Database: HyperSizer ANALYSIS METHODS 5.9.hdb
Project: Buckling Flexural-Torsional HVV
Group: 10: Integral L Panel, Composite, Thick Skin, ts/tf = 1.5, No postbuckling

This panel was designed to verify the HyperSizer solution for a composite panels. To avoid running expensive non-linear FEA, the skin was thickened so that stiffener buckling was the primary instability. The flange layup was set to enhance the torsional instability effect. Because the skin is thick in relation to the stringer, the Levy method is not applicable for this panel.

Dimensions and layups of the panel are listed in the tables below. The panel has a thick quasi-isotropic facesheet modeled using an effective laminate. The web is composed of four ±45° pairs and the flange adds eight 0° plies to the middle of the web layup.

w_{flange}	0.75"
H	1.633"
S_x	3.3"

	Layup	$t_{laminate}$ (in)	Material
Facesheet	Quasi-isotropic	0.132	AS4/3502
Web	2_[45/-45]s	0.044	AS4/3502
Flange	[45/-45/45/-45/0/0/0/0]s	0.088	AS4/3502

Figure 7 shows a representative mode shape of a 30" panel. The panel dips down in an overall flexural mode while the central stiffeners tip to the left. This mode shape is classified as a symmetric, coupled mode.

Figure 8 shows the comparison between HyperSizer and FEA for a variety of panel lengths. The Argyris method tracks the FEA solution well. Note that for short panels, the traditional panel buckling margin is very high. However, the stiffener is prone to flexural-torsional buckling which leads to a dramatic decrease in overall stability.

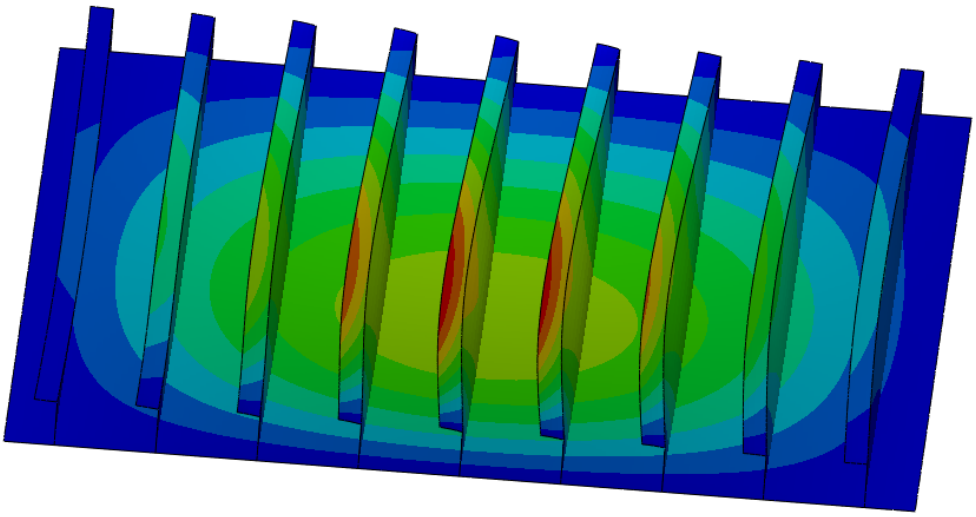

Figure 7 – Integral L, Composite - Length = 30" - Eigenvalue results. Color contours indicate the magnitude of displacement. Torsion and flexure is highly coupled.

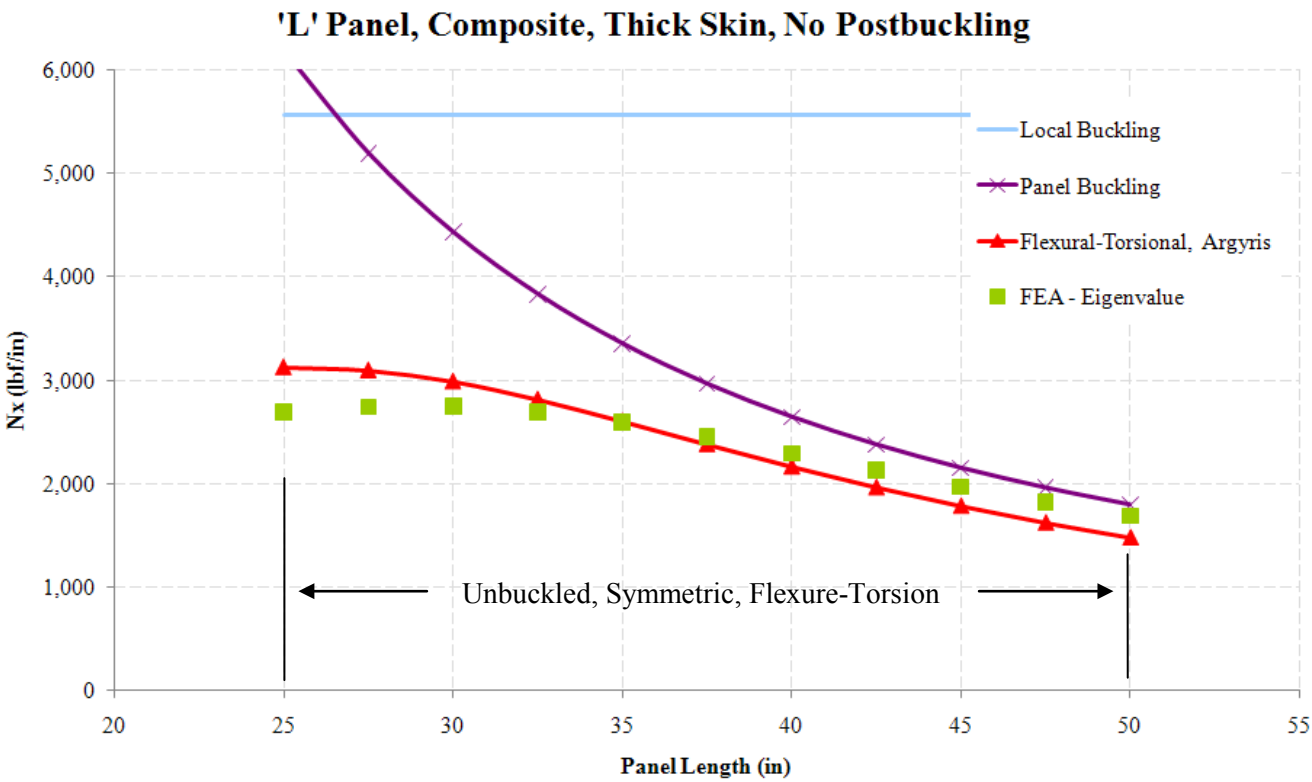

Figure 8 - FEA Verification Results for varying panel lengths. For short panel lengths, the traditional panel buckling (pure flexure) critical load is very high. However, the stiffener is prone to flexural-torsional buckling leading to a dramatic decrease in overall stability. The mode shape for all lengths is unbuckled (no local buckling), symmetric, flexure-torsion.

6 Verification Ex 4: FEA, 'I' Panel, Metallic, Bonded, Thick Skin, No Postbuckling

Database: HyperSizer ANALYSIS METHODS 5.9.hdb
Project: Buckling Flexural-Torsional HVV
Group: 20: FEA, 'I' Panel, Metallic, Bonded, Thick Skin, No Postbuckling

The following panel was chosen as an example of a symmetric stiffener. Stiffener symmetry is this context means that the plane of the web is a plane of symmetry of the stiffener. In these "symmetric" cases, flexural and torsional modes are uncoupled. Therefore, the mode return by HyperSizer will either be a pure torsional mode or pure flexural mode. Generally speaking, torsional modes will occur at shorter panel lengths.

The panel dimensions are described in the table below. Again, the facesheet is thick so stiffener buckling is critical for most panel lengths. The web was made thin compared to the free flange making this design susceptible to torsional buckling.

$t_{facesheet}$	0.18"
$t_{top\ flange}$	0.04"
t_{web}	0.08"
$t_{bot\ flange}$	0.28"
$w_{top\ flange}$	2"
$w_{bot\ flange}$	1.25"
H	1.633"
S_x	3.3"

Figure 9 shows a representative mode shape of a 20" panel. The facesheet does not deform. Instead the stiffeners tip independently of the facesheet in an antisymmetric torsional mode.

Figure 10 shows the comparison between HyperSizer and FEA for a variety of panel lengths. Because the skin is thick, the Levy method is not applicable to this panel. In general, the HyperSizer Argyris solution tracks the FEA solution well.

This panel exhibits a wide variety of buckled mode shapes. For very short panels (L < 15"), local buckling controls therefore FEA eigenvalue results do not indicate collapse at these lengths. Non-linear FEA was not run for these short panels. For medium length panels (15" < L < 45") pure torsional buckling controls. Note that for the pure torsional mode, as the panel length increases, the critical load does not necessarily decrease. Also notice that the number of stiffener half-waves increases from one to two at L = 35". The Levy method cannot capture this effect (even if the panel was thin-skinned). Finally, for long panels (L > 45"), a pure flexural mode is observed.

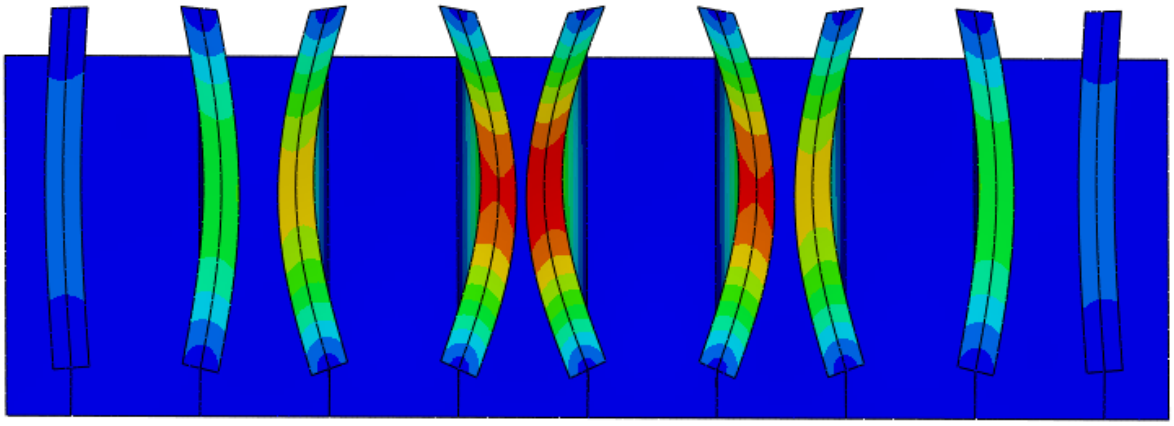

Figure 9- I Panel - Length = 20" - Eigenvalue results. Color contours indicate the magnitude of displacement. Torsion and flexure are uncoupled in this antisymmetric mode.

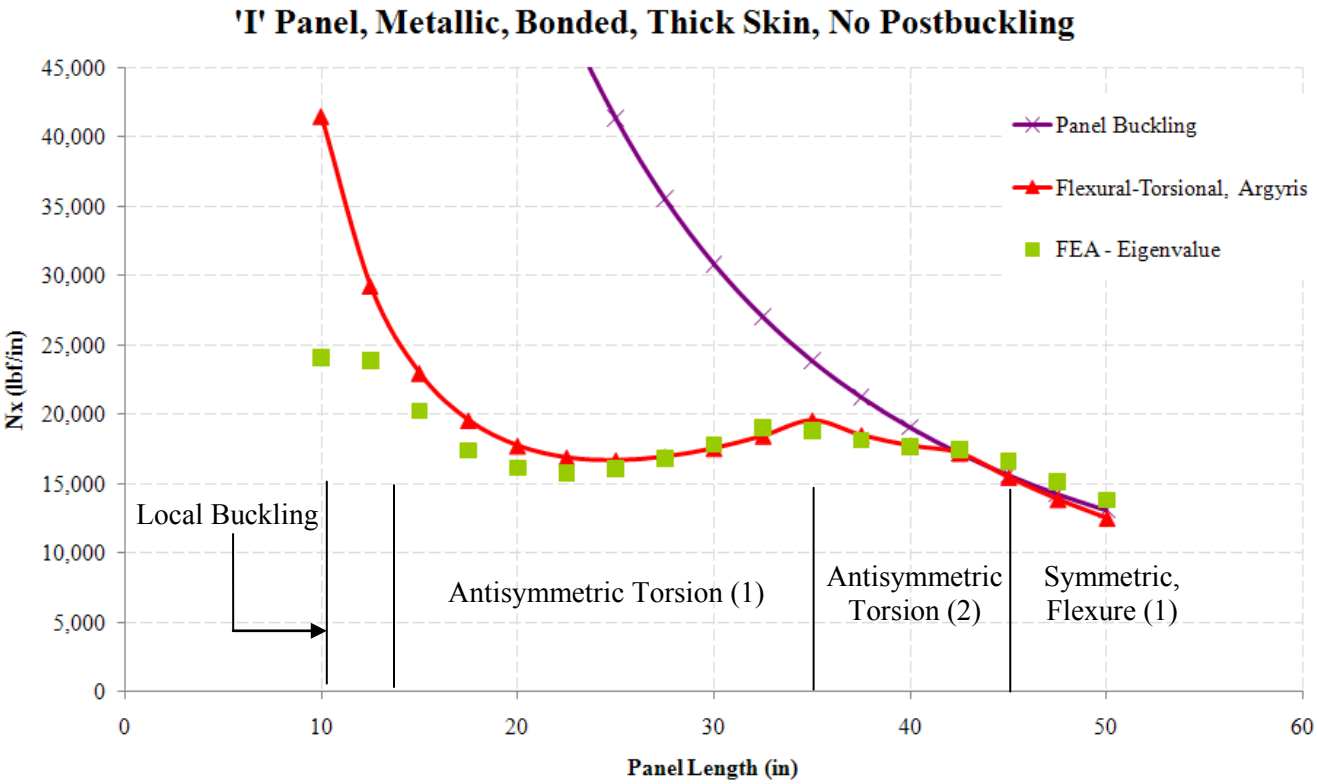

Figure 10 – I Panel FEA Verification Results for varying panel lengths. Number of stiffener half-waves are printed in parentheses. An unusual characteristic of the pure torsional mode is that the critical load does not necessarily decrease with an increase in panel length.

7 Verification Ex 5: FEA, 'Z' Panel, Metallic, Bonded, Thin Skin, Postbuckling

Database: HyperSizer ANALYSIS METHODS 5.9.hdb
Project: Buckling Flexural-Torsional HVV
Group: 30: FEA, 'Z' Panel, Metallic, Bonded, Thin Skin, Postbuckling

This panel is similar to a traditional Zee stiffened panel whose facesheet is allowed to buckle well below the limit load. Both the facesheet and the stringer are 7075 aluminum. The free flange is twice as thick as the web and the attached flange. Because local buckling is the initial instability, non-linear FEA was used to verify the postbuckling behavior of the panel. The panel is modeled as bonded in HyperSizer because FEA verifications were performed by modeling the attached flange as bonded.

$t_{facesheet}$	0.045"
$t_{top\ flange}$	0.08"
t_{web}	0.08"
$t_{bot\ flange}$	0.16"
$w_{top\ flange}$	0.93"
$w_{bot\ flange}$	1.1"
H	1.965"
S_x	5"

Figure 11 shows a representative snap shot of a 20" panel. Four panel bays were modeled in order to capture the proper rotational boundary conditions and the middle bay for flexural buckling. Bay edges are indicated by the vertical red lines. Out-of-plane constraints ($T_z = 0$) were placed on the facesheet and attached flange nodes along the bay edges to simulate the fixidity of transverse frames.

The top portion of Figure 11 shows a snapshot of the local buckling waves. The contours are the magnitude of the out-of-plane deflection. The buckling waves are seen to be slightly unsymmetric due to edge effects and other similar issues. The bottom portion of the figure shows the flexural-torsional panel buckling. The distributed blue color in the middle bay indicates a global flexural buckling normal to the skin. The stiffeners can also be seen tipping.

Finally, Figure 12 shows the curve showing the match between FEA and HyperSizer. The black dots are non-linear FEA collapse loads. The non-linear FEA result tracks the HyperSizer –Argyris result well. The Levy method is substantially conservative as compared to FEA. The HyperSizer local buckling results is very close the FEA eigenvalue result.

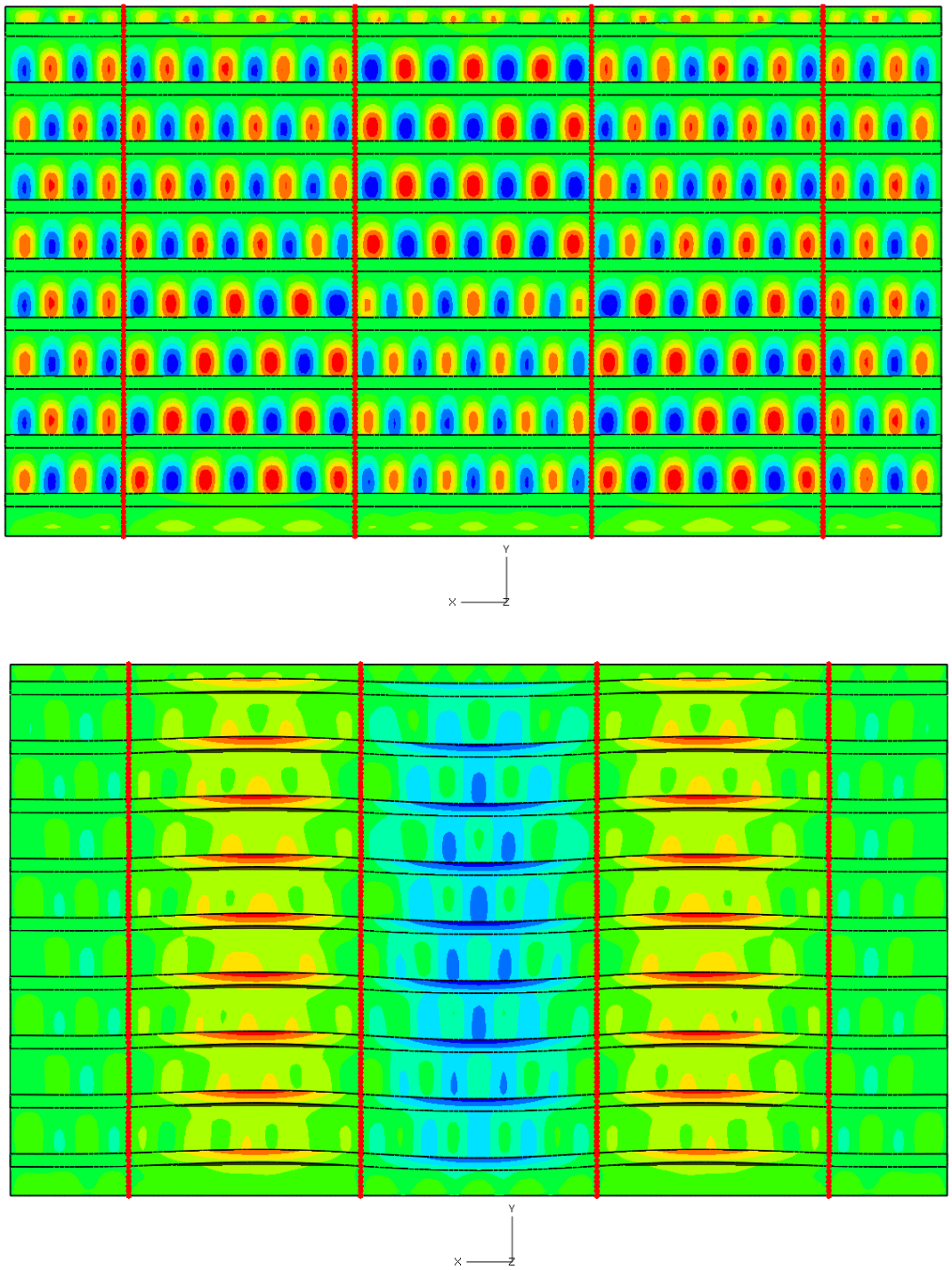

Figure 11 – Z Panel – Length = 20", Contours indicate the relative magnitude of z displacement (out-of-plane). Vertical red lines indicate bay edges of this four bay model. TOP – Initial buckling in the facesheet. The stiffeners are straight. BOTTOM – Flexural-torsional buckling. The distributed blue color in the middle bay indicates a global flexural buckling towards the skin. The stiffeners can also be seen tipping.

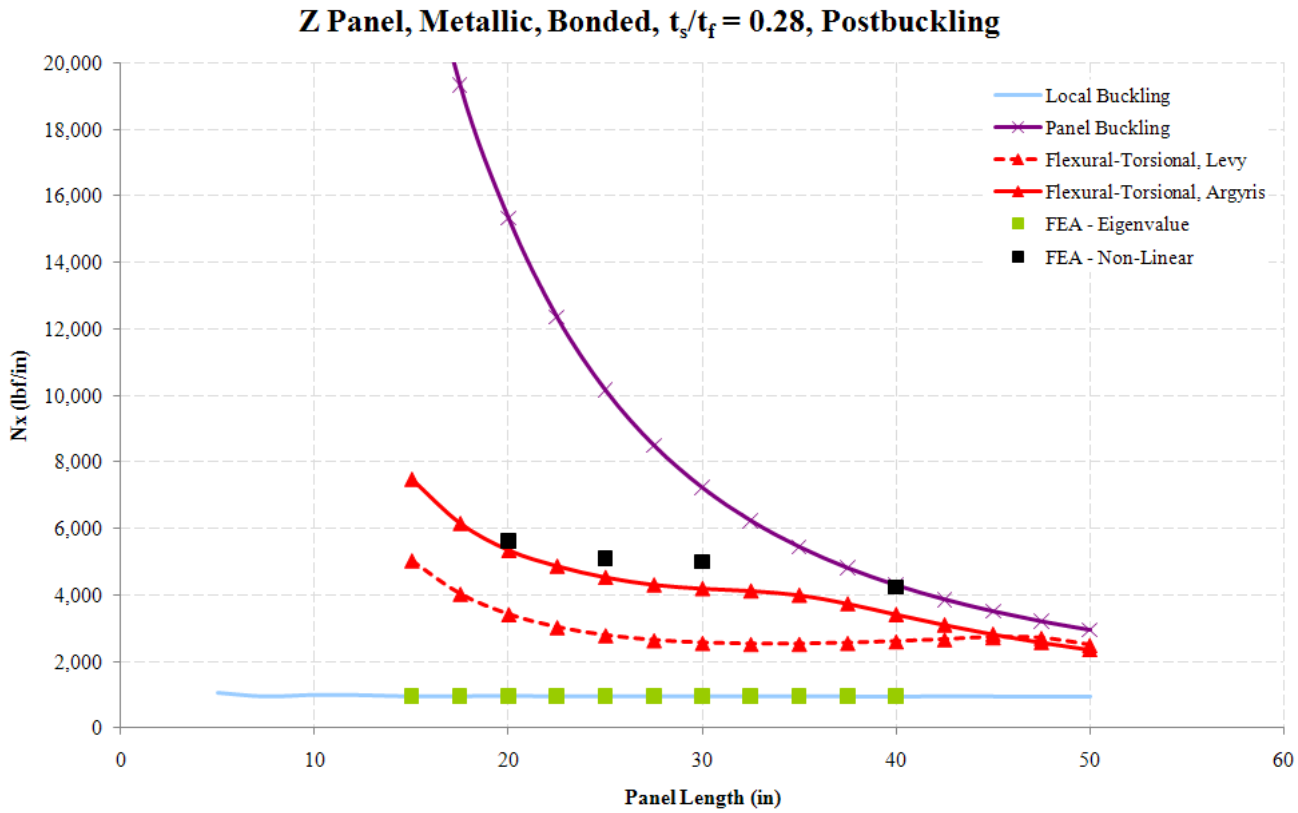

Figure 12 – Z Panel - FEA Verification Results for varying panel lengths. All modes are postbuckled, symmetric, flexural-torsional with a single stiffener half-wave. The Levy method is substantially conservative as compared to the bonded FEM.

8 Validation Ex 1: NACA Test Data, 'Z' Panel, Metallic, Fastened, Postbuckling

Database: Test Data, CF Established - Master 5.9.hdb
Project: Validation – Panel Instability – NACA-ARR-4B03

This section compares HyperSizer results with experimental results from Rossman et al. (1944) for three different lengths of the Z stiffened configuration shown above and below. Compression tests were performed on a series of aluminum alloy stiffened panels as shown in Figure 13. All of the panel Z stiffeners were formed from 0.064 in aluminum alloy sheet. Panel dimensions, loading (for HyperSizer analysis), and material properties are listed in the tables below.

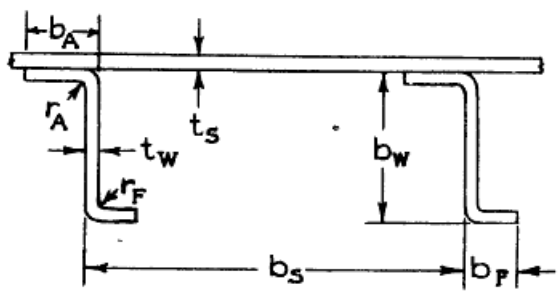

Figure 13 - Z Stiffened test panels from NACA ARR 882 4B03 (1944)

Test Panel Dimensions			
	Panel		
	1	2	3
tw	0.064"	0.064"	0.064"
bw/tw	30	30	30
bF/bw	0.2	0.2	0.2
bA/tw	8.6	8.6	8.6
tw/ts	1.0	1.0	1.0
bs/ts	50	50	50
L/bw	7.3	12.8	18.2

HyperSizer Analysis Dimensions and Load			
	Panel		
e	**1**	**2**	**3**
$t_{facesheet}$	0.064”	0.064”	0.064”
$t_{top\ flange}$	0.064”	0.064”	0.064”
t_{web}	0.064”	0.064”	0.064”
$t_{bot\ flange}$	0.064”	0.064”	0.064”
$w_{top\ flange}$	0.550”	0.550”	0.550”
$w_{bot\ flange}$	0.384”	0.384”	0.384”
H	1.984”	1.984”	1.984”
S_x	3.2”	3.2”	3.2”
L	14.02”	24.58”	34.94”
N_x	-1000 lbf/in	-1000 lbf/in	-1000 lbf/in

Material	E (Msi)	G (Msi)
Aluminum Alloy	10.3	3.9655

A comparison of HyperSizer results with NACA experimental results is shown in Figure 14. For the plotted data the NACA ARR 4B03 critical stress is the maximum average panel stress, and the HyperSizer critical stress is the average panel stress at the FTB buckling load. Since the skin local buckles for each of the three panels, all HyperSizer results were determined with local postbuckling enabled. Results are shown only for the HyperSizer Argyris method since the Levy method is known to give poor results except when the skin thickness is small compared to the stiffener thickness. The HyperSizer results are in excellent agreement with the experimental data for all three panels.

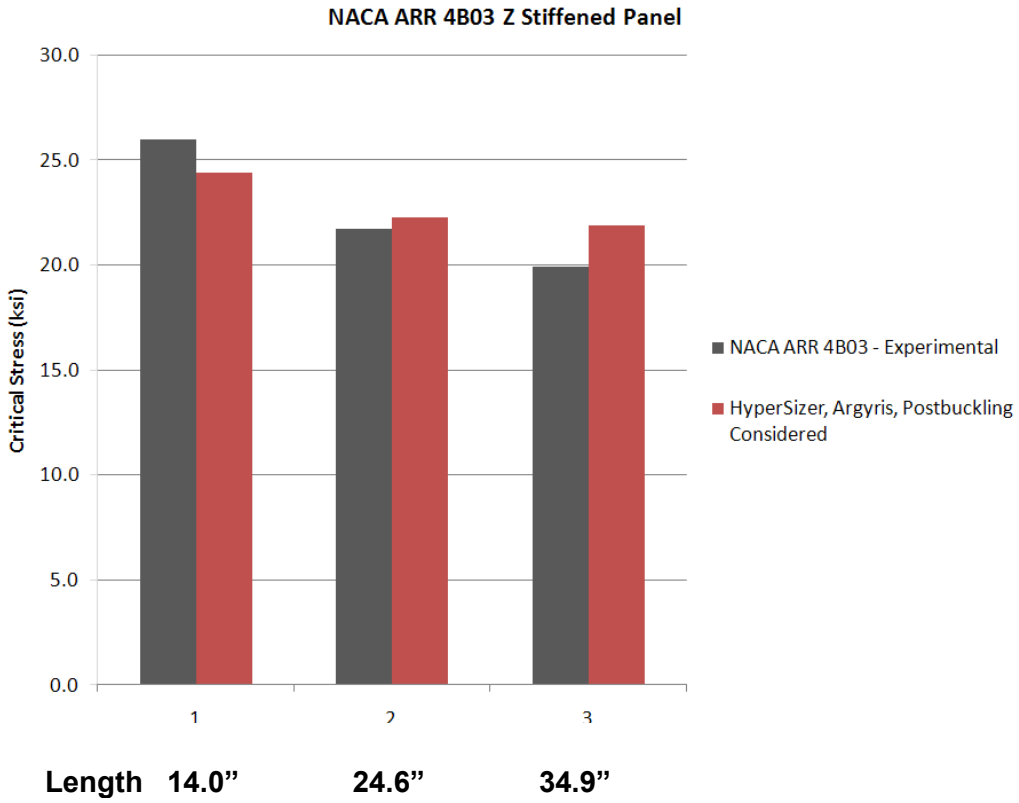

Figure 14 - HyperSizer and experimental results for NACA ARR 4B03 (1944) Z stiffened panels

9 Validation Ex 2: NACA Test Data, 'C' Panel, Metallic, Fastened, Postbuckling

Database: Test Data, CF Established - Master 5.9.hdb
Project: Validation – Panel Instability – NACA-TN-882

This section compares HyperSizer results with the experimental results from Niles (1943) for a C stiffened configuration (Panels PA-11 and PA-12) as shown above (NACA TN 882). Niles performed compression tests on a series of aluminum alloy stiffened panels. Panel dimensions, loading (for HyperSizer Analysis), and material properties are listed in the tables below. Note that panels PA-11 and PA-12 are two separate test specimens with the same dimensions and materials.

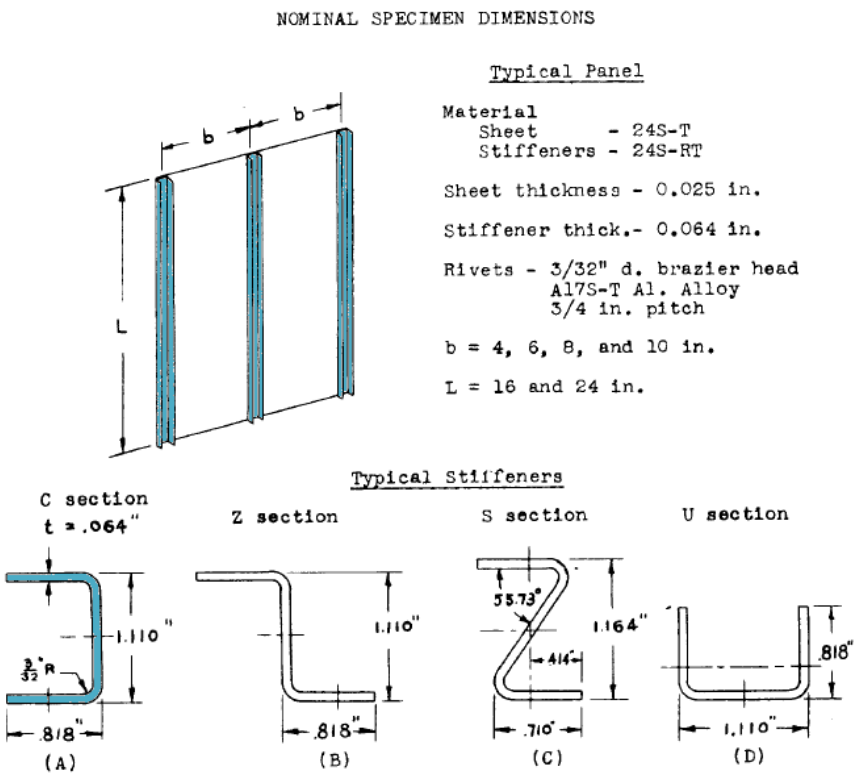

Figure 15 - C Stiffened test panels from NACA TN 882 Niles (1943)

	Panel
	PA-11 and PA-12
H	1.135”
S_x	6”
w_{flange}	0.769”
t_{flange}	0.064”
t_{web}	0.064”
$t_{facesheet}$	0.025”
L	24”
N_x	-1000 lbf/in

Material	E (Msi)	G (Msi)
Aluminum Alloy	10.3	3.9655

A comparison of HyperSizer results with NACA experimental results is shown in Figure 16. For the plotted data the NACA TN 882 critical stress is the maximum average panel stress (panel load divided by total stiffener plus skin area), and the HyperSizer critical stress is the average panel stress at the FTB buckling load. Since the skin local buckle for each of this panel, all HyperSizer results were determined with Local Post Buckling On. Results are shown for the HyperSizer Argyris and Levy methods. The HyperSizer Argyris results are in excellent agreement with the experimental data, and the HyperSizer Levy results under predict the failure stress.

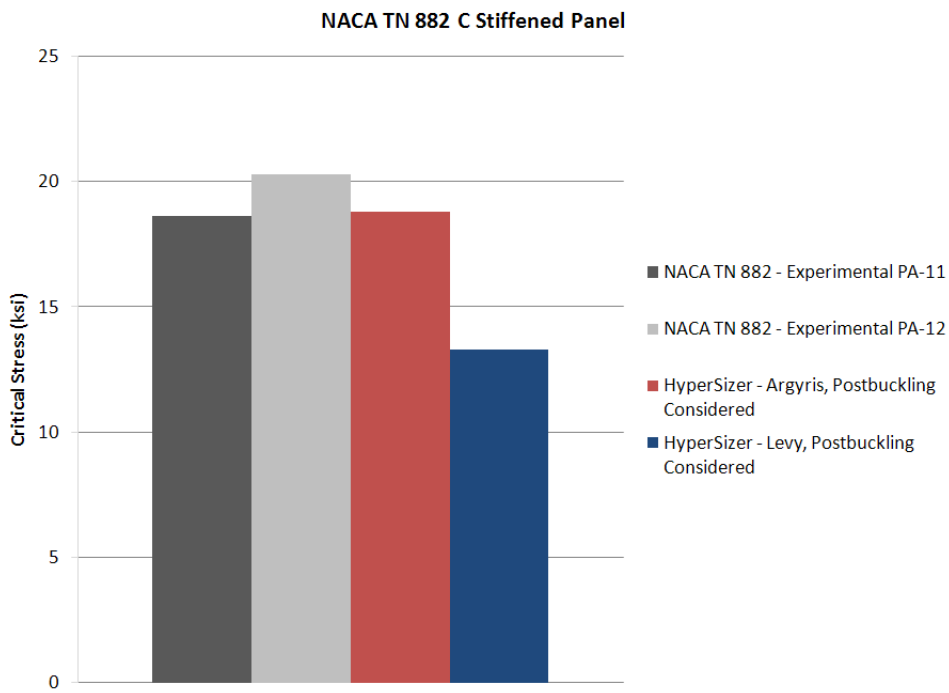

Figure 16- HyperSizer and experimental results for NACA TN 882 (1943) C stiffened panels

10 References

Argyris, J. (1954). Flexural-Torsion Failure of Panels. *Aircraft Engineering* .

Falzon, B. G., & Hitchings, D. (2007). *An Introduction to Modelling Buckling and Collapse, 2nd Edition.* NAFEMS.

Levy, S., & Kroll, W. (1948). *Primary Instability of Open-Section Stringers Attached to Sheet.* National Bureau of Standards.

Lynch, C., Murphy, A., Price, M., & Gibson, A. (2004). The computational post buckling analysis of fuselage stiffened panels loaded in compression. *Thin-Walled Structures , 42*, 1445-1464.

McCombs, W. F. (2004). *Engineering Column Analysis.* Dallas: Datatec.

Niles, A. (1943). *NACA TN 882 - Tests of Flat Panels with Four Types of Stiffeners.* Washington: NACA.

Rossman, C. A., Bartone, L. M., & Dobrowski, C. V. (1943). *NACA ARR 4B03 - Compressive Strength of Flat Panels with Z-Section Stiffeners.* Washington: NACA.

11 Appendix A: Stiffener-Frame Attachment - Pinned vs. Mousehole

The underlying theory in the Arygris and Levy method assumes that the stiffener cross-section is pinned. This means at the panel ends, the stiffener cross-section cannot translate in the plane of the cross-section, and it cannot twist (torsion) though the cross-section is allowed to warp. This assumption dictates that the buckling half-wave (both torsion and flexure) terminates at the panel-edge.

In terms of an actual panel design, this "pinned" stiffener assumption implies the that stringer is somehow attached to the transverse frame. Typical designs do not attach the stringer to the frame. Instead the stringer runs through mouseholes as shown in the figure below. If the mousehole design is used, it is conceivable that a torsional buckling wave would not necessarily terminate at the bay-edge. On the other hand, flexural buckling waves would still be assumed to terminate at the bay-edge due to the rigidity or the transverse frames.

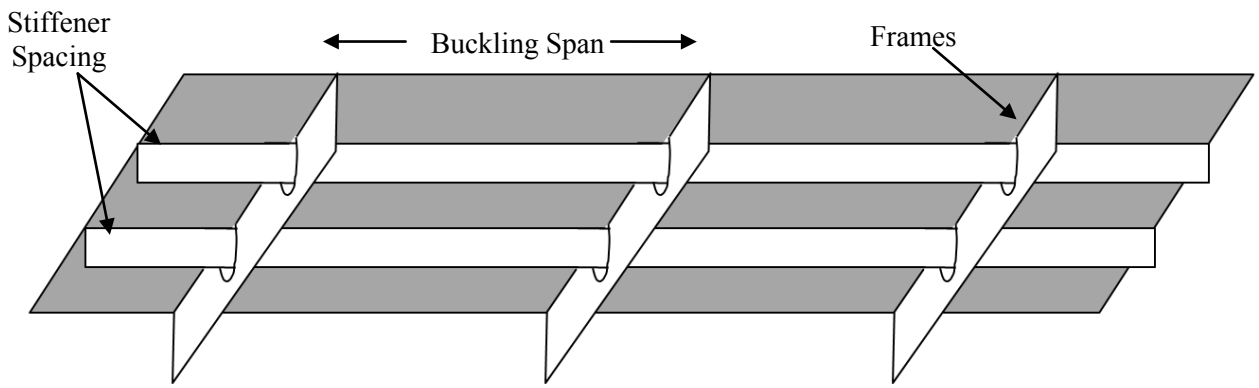

Because typical designs (mousehole) do not restrain the stringer in the same manner as assumed by the flexural-torsional method (pinned), multi-bay finite-element models were generated in HyperFemGen to quantify the potential impact on the results. Four-bay models were generated using the same thick-skin designs from Sections 5 and 6 ('L' and 'I' panel respectively).

11.1 Boundary Conditions

The static boundary conditions for the multi-bay model are the same as those described in Section 4.1.

Figure 17 shows the *buckling* boundary conditions applied for multi-bay models. Though a two-bay model is pictured, four-bay models were generated. The loaded edges are fixed. Unloaded edges are simply-supported. T_z constraints are applied on the skin nodes of the bay-edge to simulated the restraint of the transverse frames. This constraint stipulates that any flexural buckling wave must terminate at the bay-edge. T_y constraints are applied on the web and free flange nodes at the bay-edges. This constraint models the "pinned" stiffener condition assumed by the flexural-torsional method. These T_y constraints were removed to simulate the "mousehole" or "unpinned" condition.

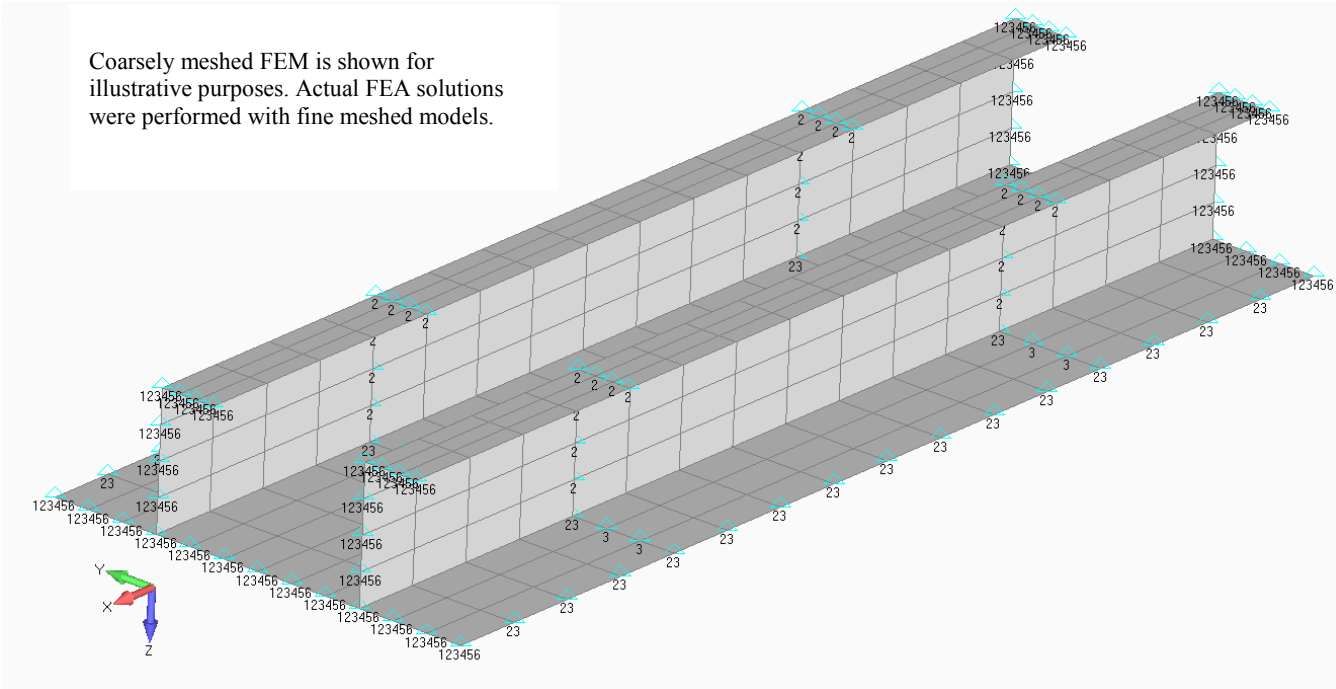

Figure 17 - Buckling conditions for a multi-bay model. The T_y constraint models the 'pinned' stiffener condtion. These constraints were removed to model the 'mousehole' or 'unpinned' condition.

11.2 'I' Panel, Metallic, Bonded, Thick Skin, No Postbuckling

The 'I' panel from Section 6 was analyzed. Because it is thick-skinned design, linear eigenvalue analysis is sufficient most panel lengths. The stiffener is symmetric. As a result, torsion and flexure are uncoupled. The stiffener boundary conditions are expected to impact the torsional mode only.

Figure 18 shows the multi-bay panel results. First, the difference between the single-bay and the four-bay model is quite signficant for the torsional modes. This is due to the edge effects brought about by fixing the loaded edges. Second, by comparing the four-bay results we see that unpinning the stiffeners tends to reduce the torsional critical stress though not by much. The flexural critical stress is not affected by the stiffener boundary conditions.

11.3 'L' Panel, Composite, Thick Skin, No Postbuckling

The 'L' panel from Section 5 was analyzed. Because it is thick-skinned design, linear eigenvalue analysis is sufficient for all panel lengths. The stiffener is not symmetric leading to a coupling of torsion and flexure. The stiffener boundary conditions are expected affect the torsional mode only. Therefore, the impact on the flexural-torsional mode is expected to be less than that of pure torsion.

Figure 19 shows the multi-bay panel results. The change in critical stress going from a single-bay to four-bay model is much less than that of the 'I' panel. Again, the unpinned stiffener condition reduces the critical stress but not significantly.

The Argyris one bay analysis approach in all cases is slightly conservative for multibay panel designs with mouseholes.

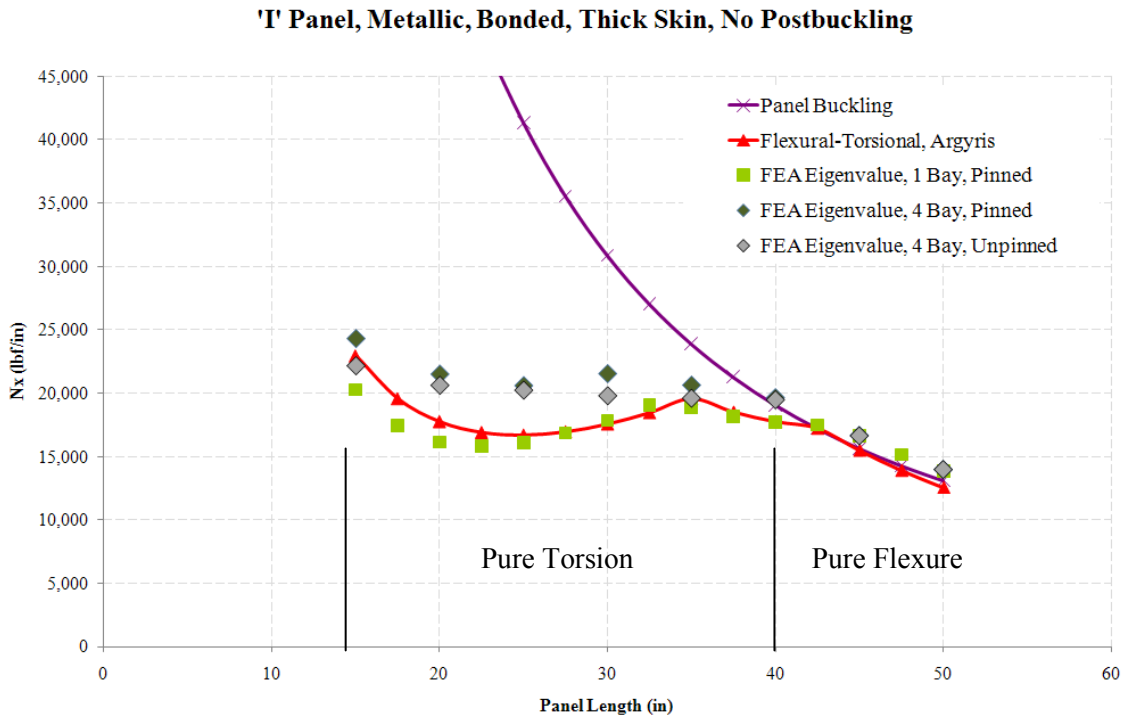

Figure 18 - FEA comparison of the pinned vs. unpinned stiffener conditions for the metallic 'I' panel. There is a signficant difference between the pinned single and four-bay models in the torsional modes. The critical torsional stress decreases slightly for the four-bay unpinned (mousehole) model.

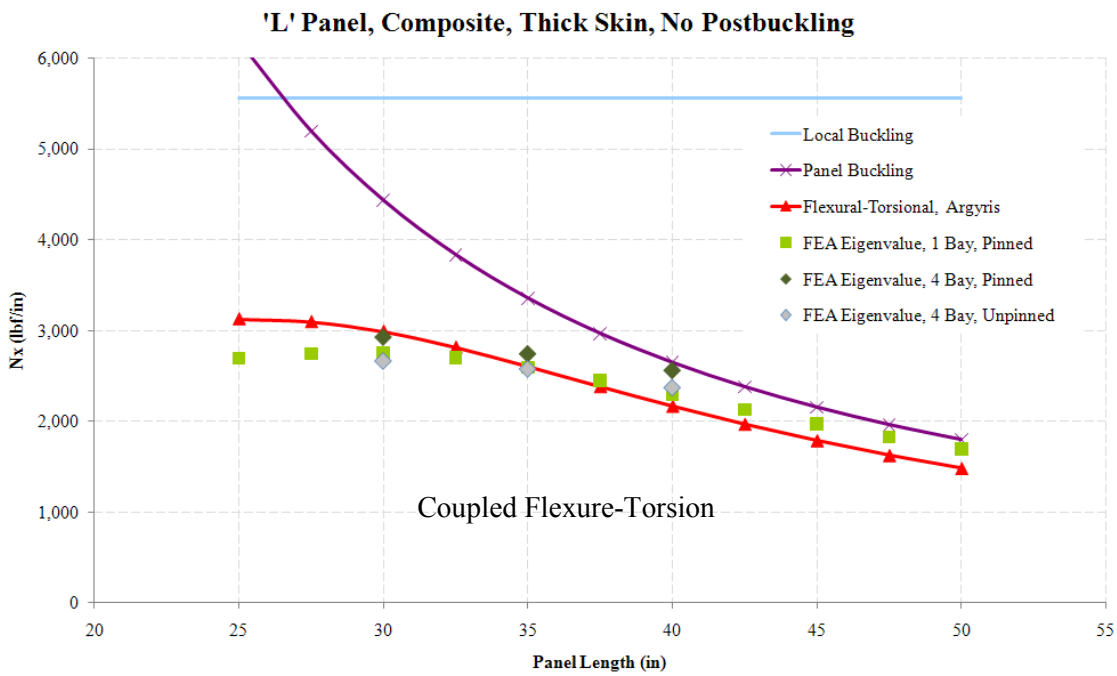

Figure 19 - FEA comparison of the pinned vs. unpinned stiffener conditions for the composite 'L' panel. Multi-bay and stiffener boundary conditions have only a moderate impact on the FEA results.